SUPPLEMENTAL DATA

WWP1 inactivation enhances efficacy of PI3K inhibitors while suppressing their toxicities in breast cancer models

Takahiro Kishikawa, Hiroshi Higuchi, Limei Wang, Nivedita Panch, Valerie Maymi, Sachem Best, Samuel Lee, Genso Notoya, Alex Toker, Lydia E. Matesic, Gerburg M. Wulf, Wenyi Wei, Motoyuki Otsuka, Kazuhiko Koike, John G. Clohessy, Yu-Ru Lee, and Pier Paolo Pandolfi

Supplemental Figure Legends

Supplemental Figure 1 - 8

Supplemental Table 1

Supplemental Figure legends

Supplemental Figure 1. PTEN was dissociated from the plasma membrane upon PI3K inhibition through the membrane recruitment of WWP1.

(A) Negative loading controls of subcellular fractionation in MDA-MB-231 cells treated with multiple PI3K inhibitors. Related to Fig. 1C. **(B)** Representative immunofluorescent images of PTEN subcellular localization. MDA-MB-231 cells stably expressing shWWP1 were treated with BKM120 for 12 h. Bar, 10 μm. **(C)** Binding of WWP1 to PTEN in MCF7 and MDA-MB-

231 cells upon PI3K inhibitor treatment. Total lysate from each cell was immunoprecipitated with anti-PTEN beads 24 h after the treatment with 1 μM of PI3K inhibitors. **(D)** PIP binding assay for WWP1. 293T cells were transfected with MYC-WWP1 and subsequently immunoprecipitated with $PI(4,5)P_2$, $PI(3,4,5)P_3$, or control beads.

Supplemental Figure 2. *WWP1* depletion improved the efficacy of BKM120 in a PTEN-dependent manner.

(A) Dose response curve of BKM120 in indicated breast caner cell lines. The upper panels show cells in which PTEN is expressed and the lower panels shows cell lines where PTEN is not expressed. Each dot shows mean ± SD of duplicated assay. **(B)** Dose response curve of BKM120 in MDA-MB-468 cells stably expressing Flag-PTEN and shWWP1. Each dot shows mean ± SD of triplicated assay. **(C)** Evaluation of AKT activity in MDA-MB-468 cells upon PTEN expression in *WWP1* deficient setting. Cells were treated with 1 μM of BKM120 for 48 h and subjected to WB.

Supplemental Figure 3. WWP1 was upregulated in isogenic resistant cells and its inhibition improved the sensitivity to PI3K inhibitors.

(A) and **(B)** Dose response curve of BKM120 and IC_{50} values in isogenic resistant MDA-MB-231 **(A)** and MCF7 **(B)** cells. Each dot is shown as mean ± SD in duplicated assay. **(C)** Relative expression levels of WWP1 mRNA in isogenic resistant cells. Each plot is shown as mean ± SD in triplicated assay (*$p < 0.05$, **$p < 0.01$, one-way ANOVA followed by Tukey-Kramer multiple comparisons test). **(D)** ChIP qPCR assay to evaluate MYC binding capacity on *WWP1*

promotor region. Chromatin fractions of MDA-MB-231 parental/resistant cells were immunoprecipitated with anti-Myc or H3 beads and subjected to qPCR. JunB served as positive control for MYC binding site. Data are shown as mean ± SD (**P < 0.01, ***P < 0.005, triplicate experiments, Student's *t* test). **(E)** Membrane and cytosol fractions of MCF7 cells overexpressing HA-WWP1. Cells were treated with 1.0 μM of BYL719 for 48 h and subjected to WB. LRP6 and HSP90 served as membrane and cytosol markers, respectively. **(F)** Analysis of AKT and S6 activity in MCF7 resistant HD cells upon stable expression of WWP1 shRNA. Cells were treated with 1.0 μM of BYL719 for indicated time and subjected to WB.

Supplemental Figure 4. Combination therapy with PI3K and WWP1 inhibitor synergistically suppressed cell growth in a PTEN dependent manner.

(A) and **(B)** 3-D plot of synergy score and dose response curve of BYL719 in MCF7 parental and resistant HD cells in combination with I3C treatment. Each dot is presented as mean ± SD of triplicated experiments. **(C)** 3-D plot of synergy score and dose response curve of combination therapy of BKM120 and I3C in MDA-MB-468 cells. Each dot is presented as mean ± SD of duplicated experiments.

Supplemental Figure 5. AMPKα2 isoform was specifically activated by WWP1 inhibition in the muscle tissue upon PI3K inhibition.

(A) Normalized mRNA expression levels of AMPKα1 and AMPKα2 in multiple human normal tissues. Data was obtained from the Human Protein Atlas database (https://www.proteinatlas.org/). **(B)** and **(C)** Analysis of the expression profile of AMPKα

isoforms in mouse tissues **(B)** and human breast cancer cell lines **(C)**. Bar plots are shown as mean ± SD of triplicated experiments. **(D)** Assessment of the phosphorylation of AMPKα in 293T cells. Cells were transfected with wild-type and catalytically inactive (CA) MYC-WWP1, and HA-AMPKα2 upon treatment with 1.0 μM BKM120 for 3 h and subjected to WB. **(E)** Evaluation of AMPK expression in C2C12 cells upon BKM120 and I3C combination treatment. Differentiated C2C12 cells were pretreated with I3C (150 μM) for 3 days followed by BKM120 (2.0 μM) treatment for 24 h. **(F)** Assessment of AMPK activity in MCF7 cells upon stable expression of shWWP1. Cells were treated with 1.0 μM of BYL719 for 24 h. **(G)** Intracellular ADP/ATP ratio of C2C12 cells upon stable expression of shWWP1. Cells were treated with 1.0 μM of BKM120 for 2h (n = 4, one-way ANOVA followed by Tukey-Kramer multiple comparisons test). *$p < 0.05$, **$p < 0.01$.

Supplemental Figure 6. Reduction of glucose uptake upon PI3K inhibitor treatment was restored by WWP1 inhibition through the activation of AMPKα2.

(A) Relative expression levels of pAMPK in quadriceps muscle (representative image in Fig. 3G). Measured intensity of the bands in WB was normalized by total AMPK with Image J software (n = 5, one-way ANOVA followed by Tukey-Kramer multiple comparisons test). **(B)** Assessment of cell surface GLUT4 upon BKM120 treatment and *Wwp1* silencing in C2C12-Myc-GLUT4-mCherry cells. Histograms show the representative distribution of Myc-tag-GLUT4 intensity in indicated cells measured by flowcytometry. **(C)** Longitudinal measurement of blood glucose levels upon BKM120 and AMPK inhibitor (Compound C) treatment. Compound C (CC) or PBS were administrated intraperitoneally into $Wwp1^{-/-}$ and $Wwp1^{+/+}$ mice 30 min before peroral treatment of BKM120 (50 mg/kg). Data represent mean ± SD of blood

glucose levels (n = 6 in each arm, two-tailed Student *t* test). **(D)** Glucose uptake in MDA-MB-231 cells upon BKM120 treatment. Cells upon stable expression of WWP1 shRNA were treated with BKM120 for 17h along with starvation. Each plot shows mean ± SD of triplicated assay (one-way ANOVA followed by Tukey-Kramer multiple comparisons test). *p < 0.05, **p < 0.01.

Supplemental Figure 7. Combination therapy with I3C enhanced the efficacy of PI3K inhibitor.

(A) Soft agar colony formation assay with MDA-MB-231 cells treated with multiple PI3K inhibitors. Cells with the expression of Scramble (shScr) or WWP1 shRNA (shWWP1) were seeded in agarose gel and treated with indicated drugs for 28 days (n = 3 each). **(B)** and **(C)** Soft agar colony formation assay of MDA-MB-231 parental (**B**) and resistant (**C**) cells. Each plot is shown as mean ± SD of triplicated assays. **(D)** Representative images of immunohistochemistry staining with Ki-67 in tumor xenograft model. Scale bar represents 100 μm. Bar plot shows mean percentage ± SD of Ki-67 positive cells in three independent eye fields. **(E)** Activation of caspase-3 in xenograft tumors. Dissected tumor derived from MDA-MB-231 resistant cells in each treatment arm was subjected to WB. Relative expression levels of cleaved caspase-3 (CC3) were plotted with mean value ± SD (triplicated). *p < 0.05, **p < 0.01. One-way ANOVA followed by Tukey-Kramer multiple comparisons test was used in **A**, **B**, **C**, **D**, and **E**.

Supplemental Figure 8. Combination therapy with I3C enhanced PI3K inhibitor efficacy concomitantly mitigating drug induced hyperglycemia.

(A) and **(B)** Tumor xenograft assay was performed with subcutaneous implantation of MCF7 cells. Mice were treated orally with vehicle, BYL719 (20 mg/kg), I3C (100 mg/kg), or combination of them 5 day a week from 7 days after implantation. Tumors were extracted at day 52 followed by weight measurement. Data are shown as mean ± SD in weight. (n = 8 in BYL719 + I3C arm and n = 10 in the other arms). **(C)** and **(D)** Blood insulin measurement of mice bearing MDA-MB-231 resistant **(C)** or MCF7 **(D)** xenografts upon indicated treatment (n = 5 per group). **(E)** Blood insulin levels of mice bearing PDX TNBC tumors. Peripheral blood was obtained 3 h after the treatment at the day of euthanasia (n = 7 in vehicle arm and n = 6 in the other arms). *p < 0.05, **p < 0.01, and ***p < 0.001. One-way ANOVA followed by Tukey-Kramer multiple comparisons test was used in **A**, **C**, **D**, and **E**.

Supplemental Figure 1

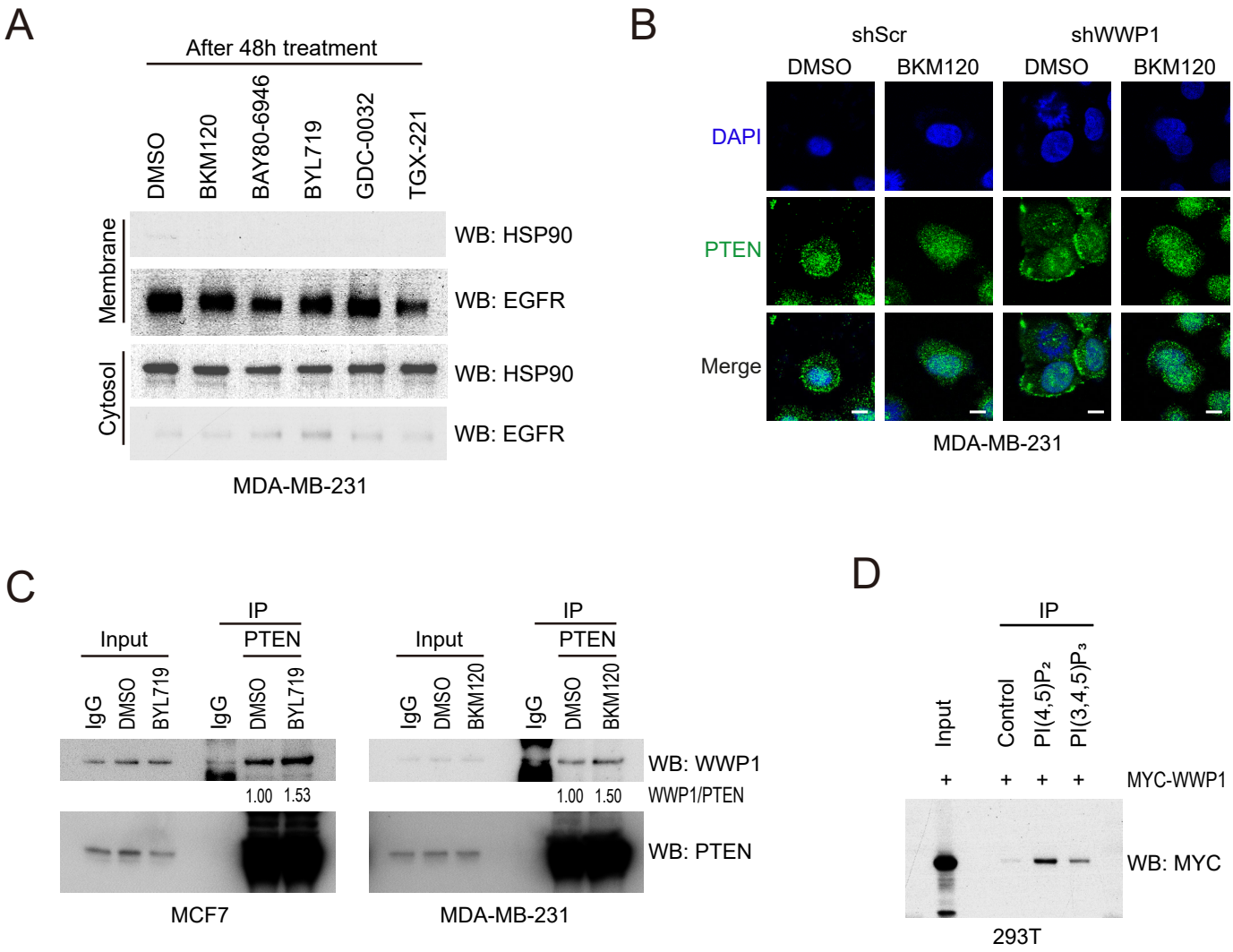

Supplemental Figure 2

A

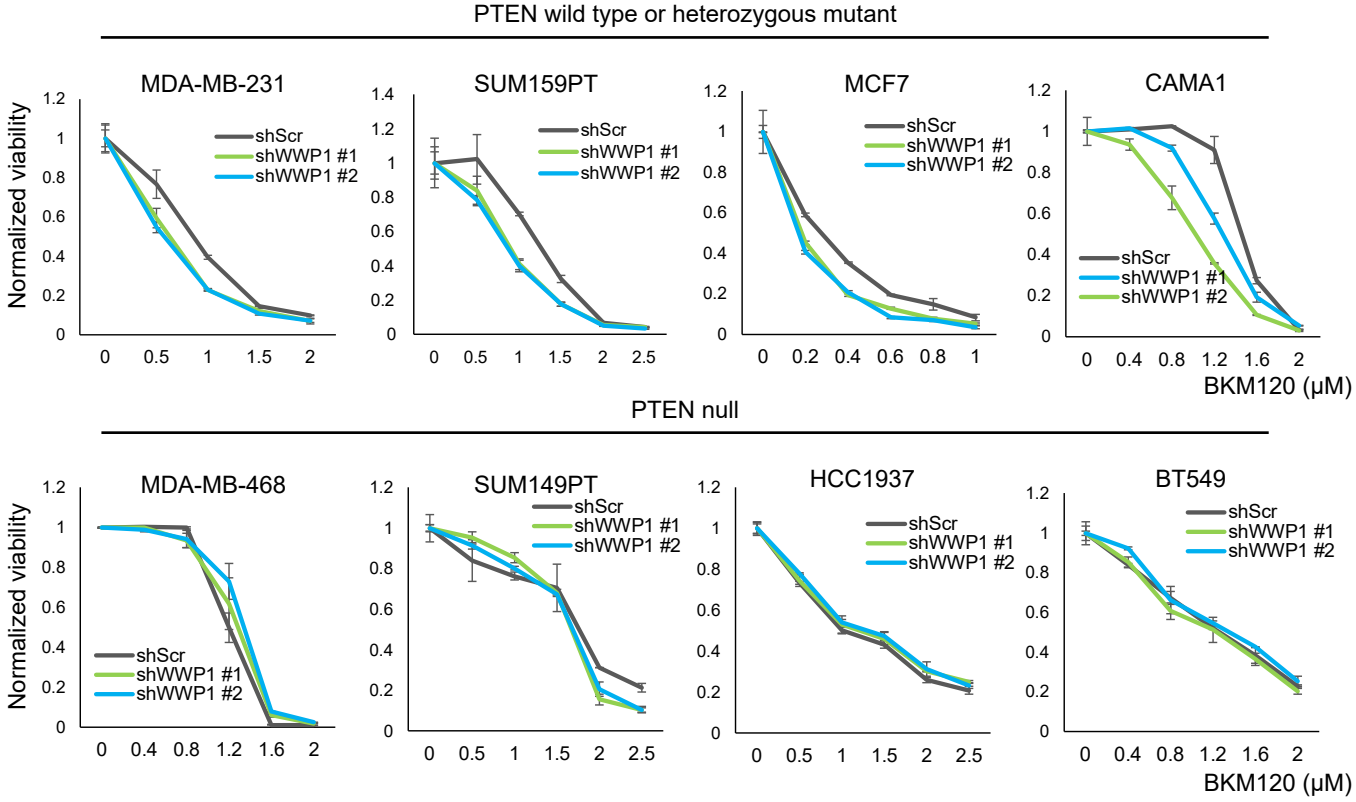

B

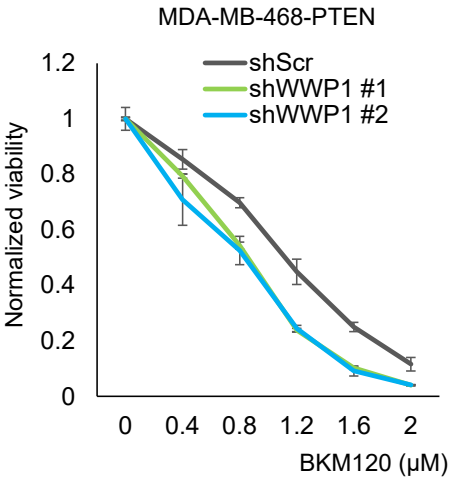

C

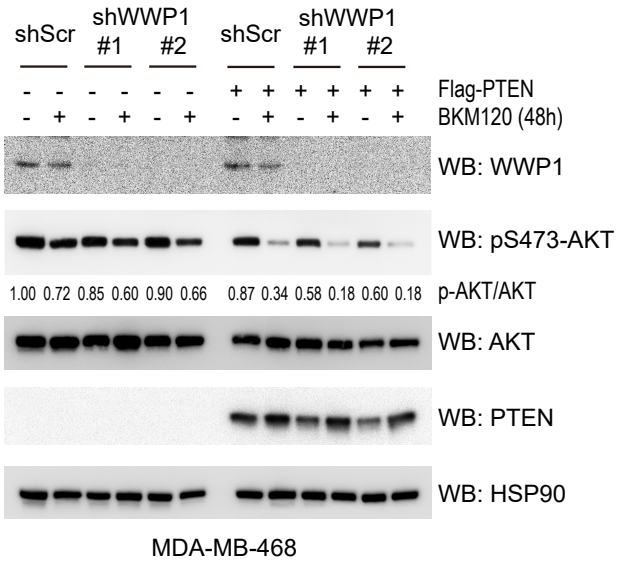

Supplemental Figure 3

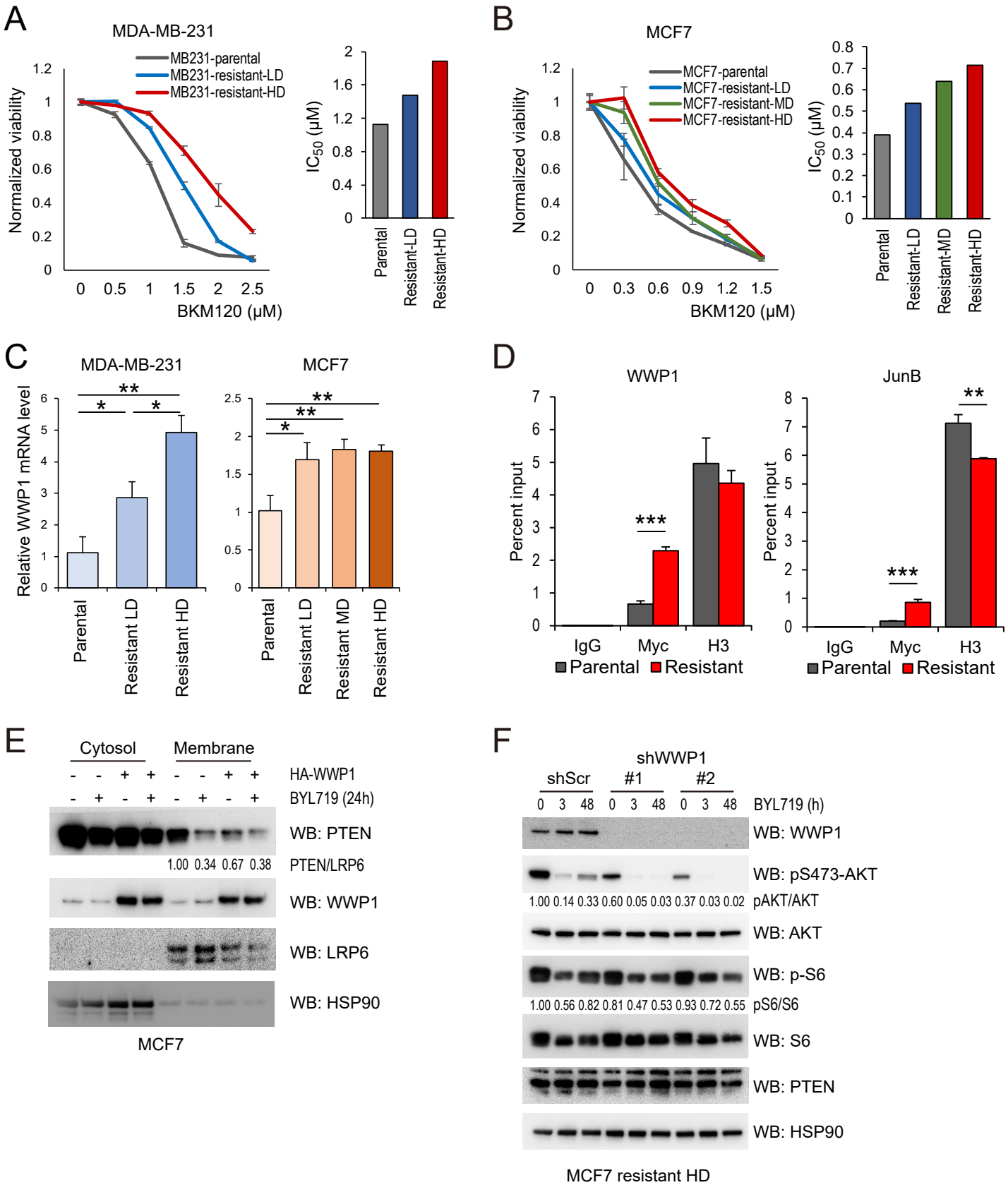

Supplemental Figure 4

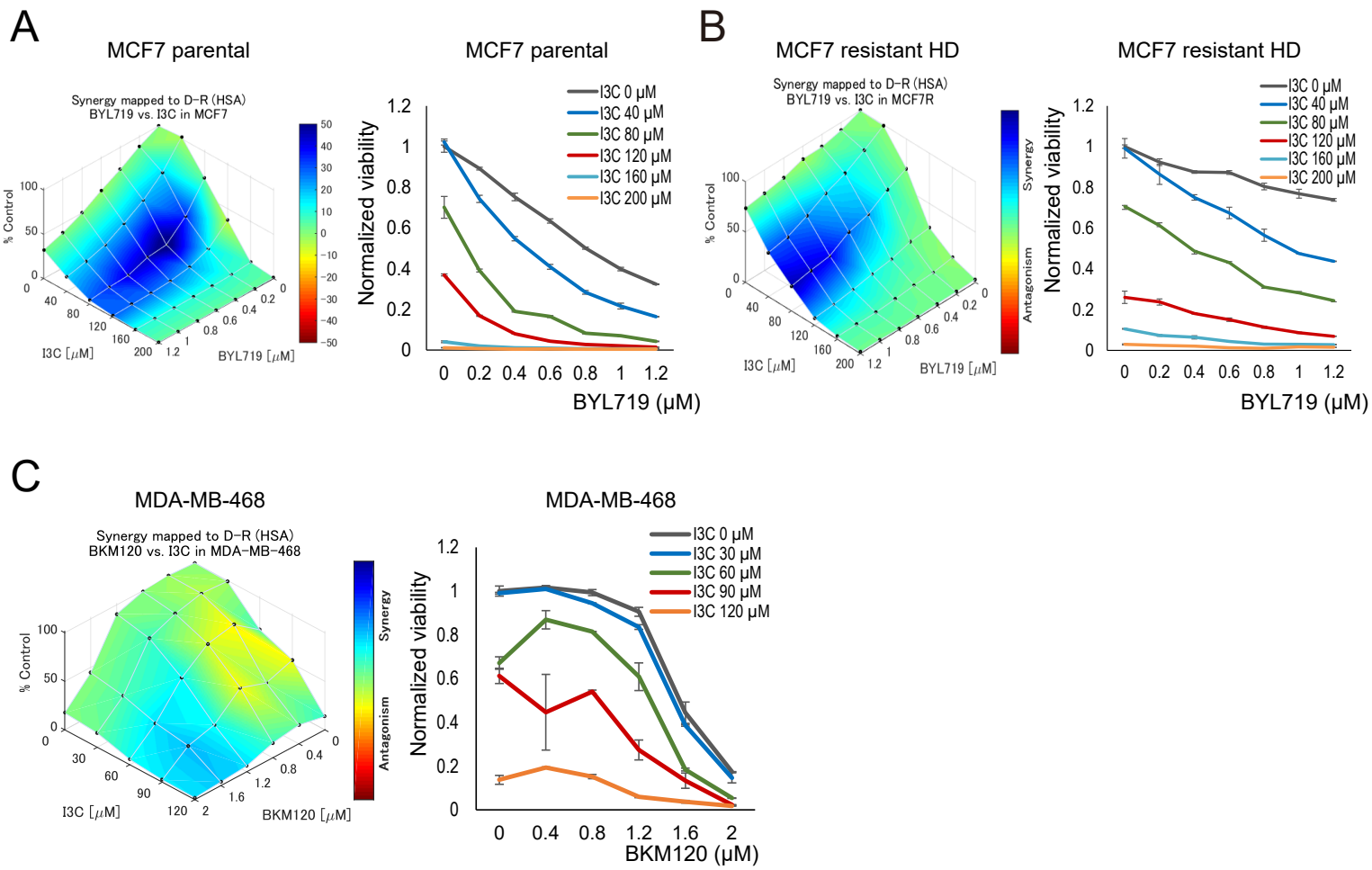

Supplemental Figure 5

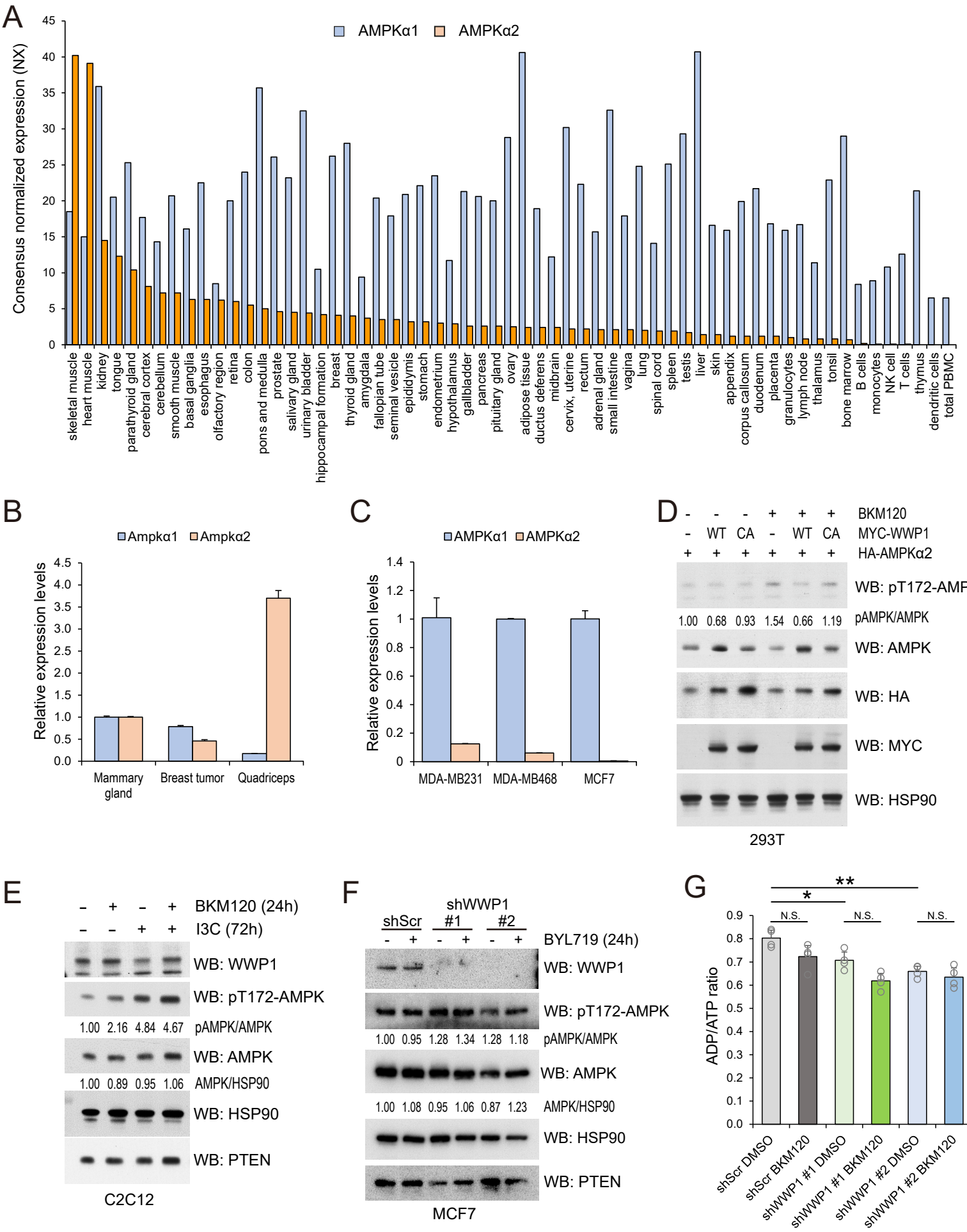

Supplemental Figure 6

A

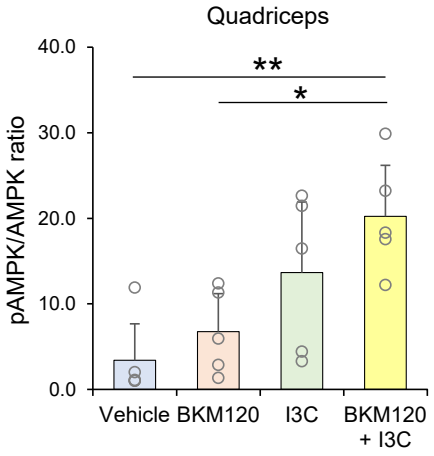

B

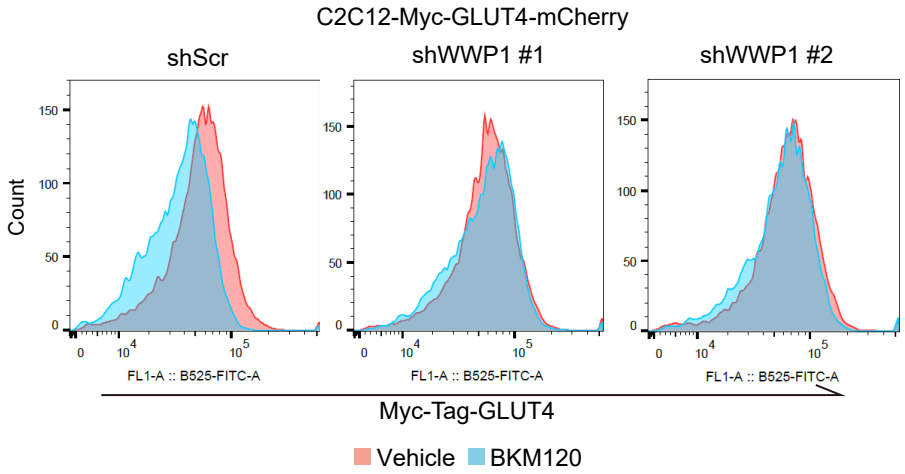

C

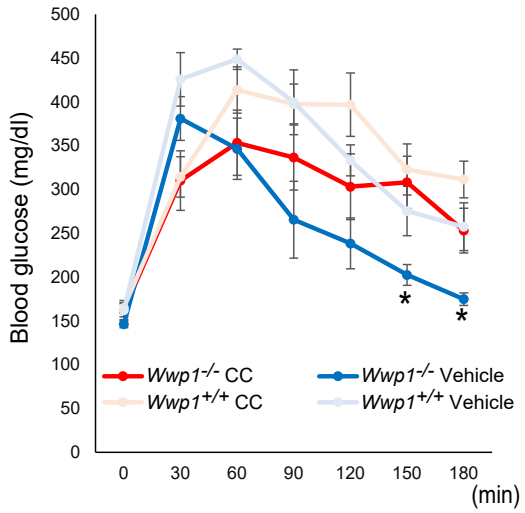

D

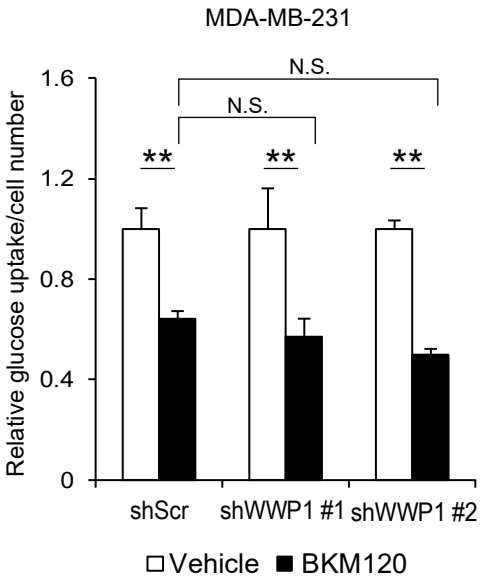

Supplemental Figure 7

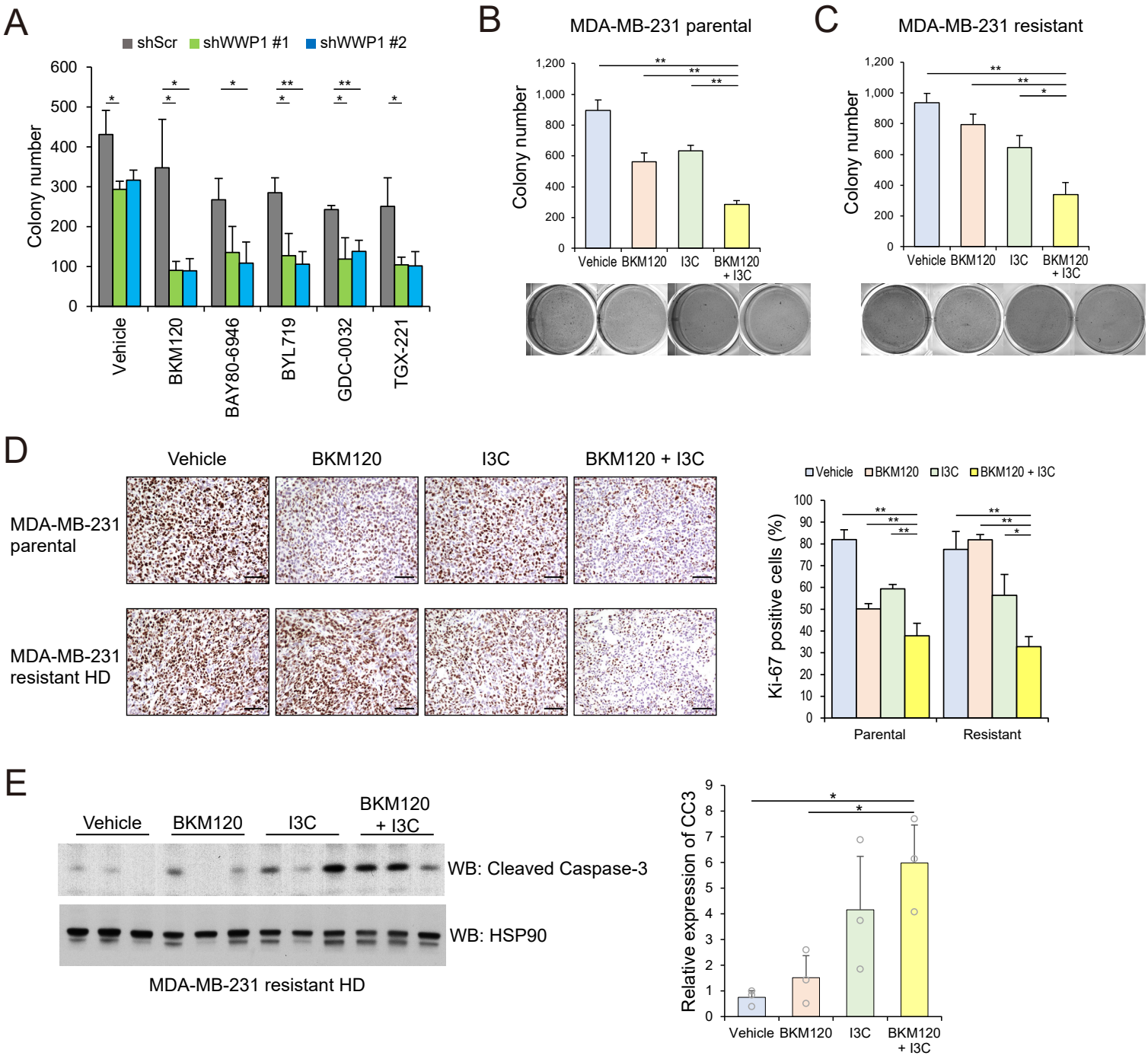

Supplemental Figure 8

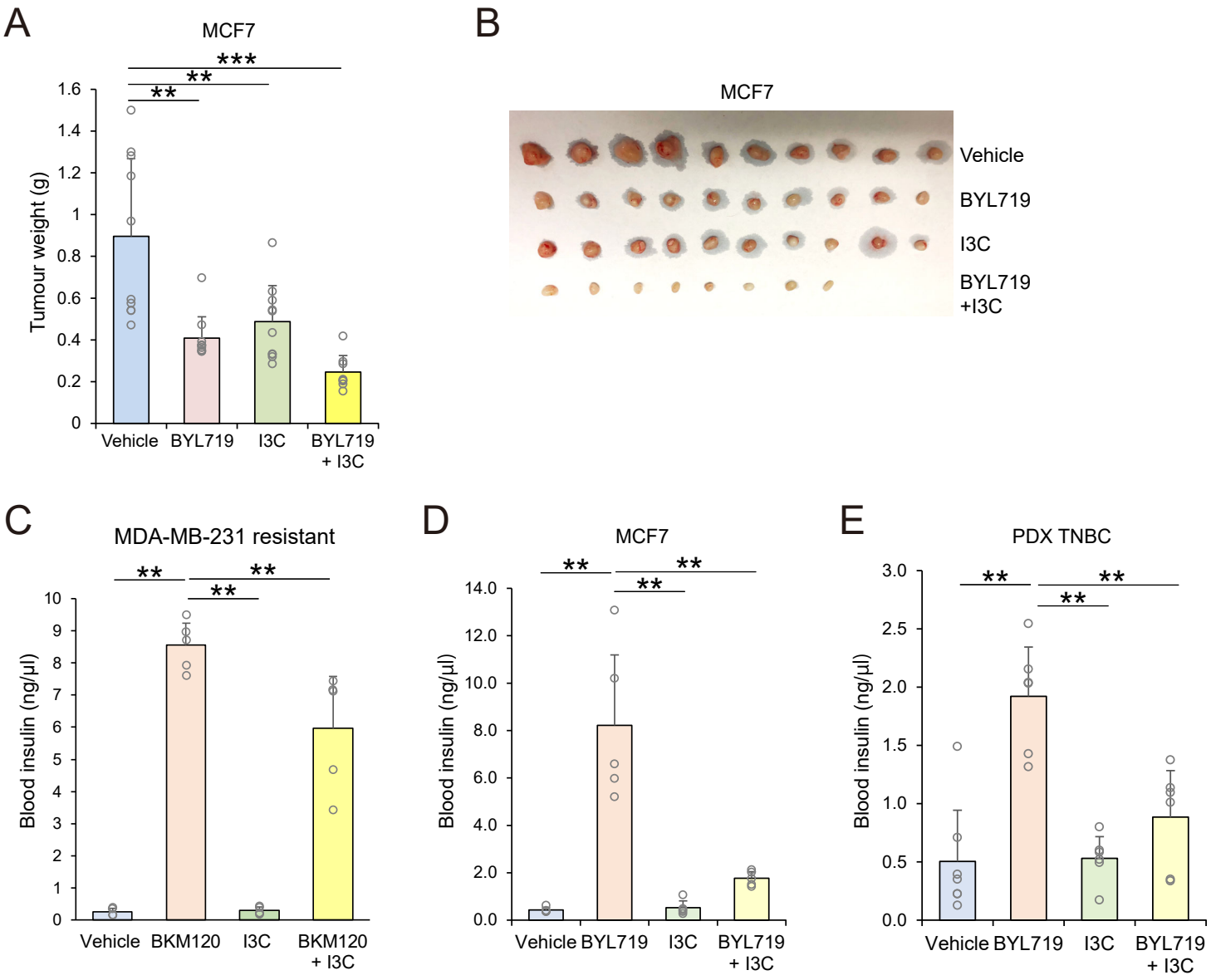

Cell line	MDA-MB-231	SUM159PT	MCF7	CAMA-1	MDA-MB-468	SUM149PT	HCC1937	BT549
Lineage subtype	TNBC	TNBC	ER+, PR+, HER2-	ER+ HER2+	TNBC	TNBC	TNBC	TNBC
Molecular subtype	Basal B	Basal B	Luminal	Luminal	Basal A	Basal B	Basal A	Basal B
PTEN	WT	WT	WT	p.D92H, p.T277fs	c.G253+1T	Epigeneticall y silenced	Homozygous deletion	p.V275fs*
PIK3CA	WT	H1047R	E545K	WT	WT	WT	WT	WT
AKT1	WT	WT	WT	WT	WT	WT	WT	WT
AKT2	WT	WT	WT	WT	WT	WT	WT	WT
AKT3	WT	WT	WT	WT	WT	WT	WT	WT
TSC1	WT	WT	WT	WT	WT	WT	WT	WT
TSC2	WT	WT	WT	WT	WT	WT	WT	WT
MTOR	WT	WT	WT	WT	WT	WT	WT	WT
RHEB	WT	WT	WT	WT	WT	WT	WT	WT
TP53	p.R280K	p.157_158insL	WT	p.R280T	p.R273H	p.M237I	p.R306*	p.R249S
RB1	WT	p.K530N	WT	WT	c.265_2787del2523	WT	c.2222_2326-20del	WT
RAS	KRAS p.G13D	HRAS p.G12D	WT	WT	WT	WT	WT	WT
BRAF	p.G464V	WT	WT	WT	WT	WT	WT	WT
BRCA1/2	WT	WT	WT	WT	BRCA2 p.M965I	BRCA1 p.N723fs	WT	WT

Supplemental Table 1. **Subtype and mutational landscape in breast cancer cell lines tested in this study.**

Mutational information was obtained from COSMIC database (www.sanger.ac.uk/genetics/CGP/cosmic/). TNBC subtype classification according to Lehmann et al. (40).